Supporting Information

Synergistic decarboxylation over Ce-doped Na/SiO_2 facilitating functionalized monomer production from furfural for manufacturing polymers

Yanlong Qi,[a] Ruilin Feng,[a,b] Shijun Liu,[a,b] Long Cui,[a] Quanquan Dai [a] and Chenxi Bai [a,b,*]

[a] Key Laboratory of High-Performance Synthetic Rubber and its Composite Materials, Changchun Institute of Applied Chemistry, Chinese Academy of Sciences, # 5625, Renmin Road, 130022, Changchun, China.

[b] University of Science and Technology of China, # 96, JinZhai Road, 230026, Hefei, China.

Email: baicx@ciac.ac.cn

Experimental section

MgAl, ZnAl, CaMg and MgZr were prepared according to reported work.[1, 2] Typically, $Mg(NO_3)_2 \cdot 6H_2O$ and $Al(NO_3)_3 \cdot 6H_2O$ with Al/Mg molar ratio of 1, 2 and 3 were respectively dissolved in deionized water (the total metal ion concentration of 1 $mol \cdot l^{-1}$), followed by the slow addition of alkaline solution of K_2CO_3 (0.5 $mol \cdot l^{-1}$) and KOH (3 $mol \cdot l^{-1}$) under continuous stirring until pH = 9.5 ± 0.5 was attained. The precipitate was aged at room temperature for 5 h, filtrated and washed several times with water. The obtained samples were dried at 120 ℃ for 12 h, and referred to as MgAl1-2, MgAl1-3 and MgAl1-4, respectively. Similarly, ZnAl1-2, CaMg1-2, CaMg1-3, CaMg1-4, MgZr1-2, MgZr1-3, MgZr1-4 were prepared by using $Zn(NO_3)_2 \cdot 6H_2O$, $Mg(NO_3)_2 \cdot 6H_2O$, $Ca(NO_3)_2 \cdot 6H_2O$, $Al(NO_3)_3 \cdot 6H_2O$. All these sample were calcined in air at 500 ℃ for 4 h prior to use. As comparison, ZnO, MgO and CaO were prepared by calcining $Zn(NO_3)_2 \cdot 6H_2O$, $Mg(NO_3)_2 \cdot 6H_2O$, $Ca(NO_3)_2 \cdot 6H_2O$ in air at 500 ℃ for 4 h.

Tables and Figures

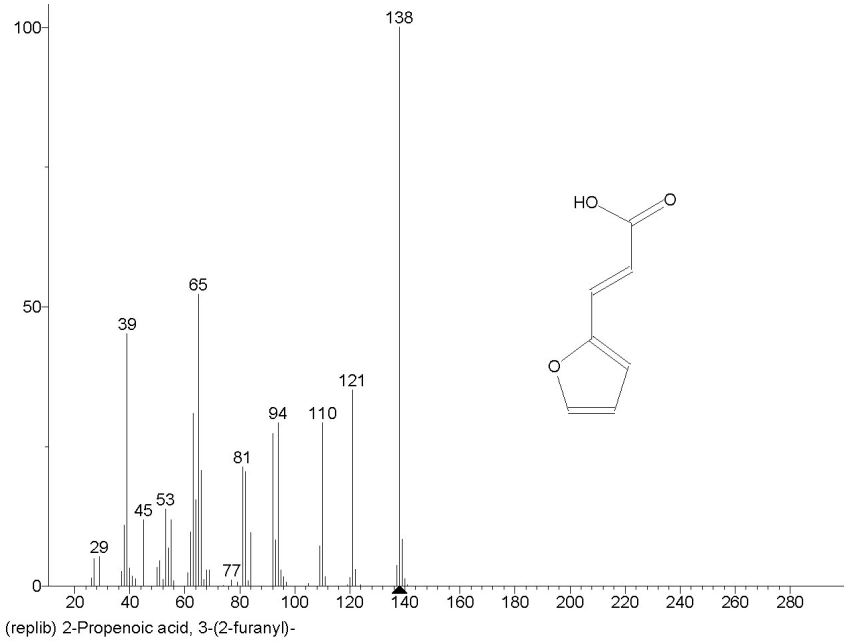

Figure S1. Mass spectrum fragmentation pattern of furylacrylic acid

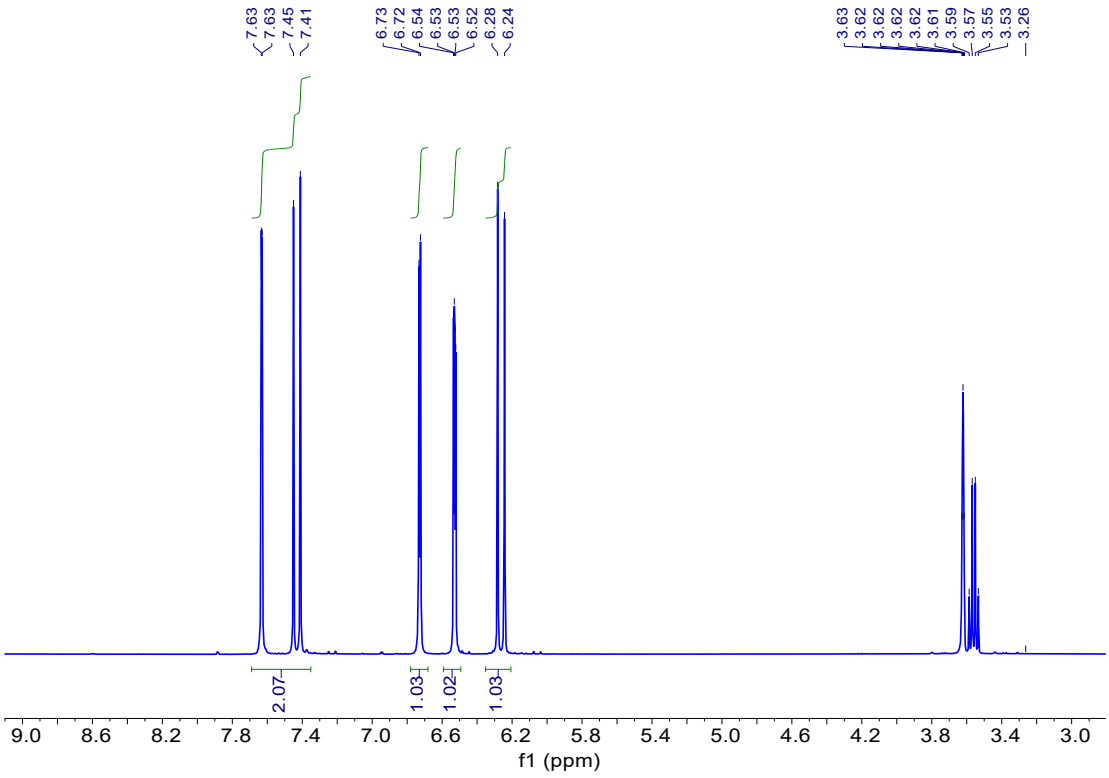

Figure S2. ^{1}H NMR of furylacrylic acid (400 MHz, $CDCl_3$)

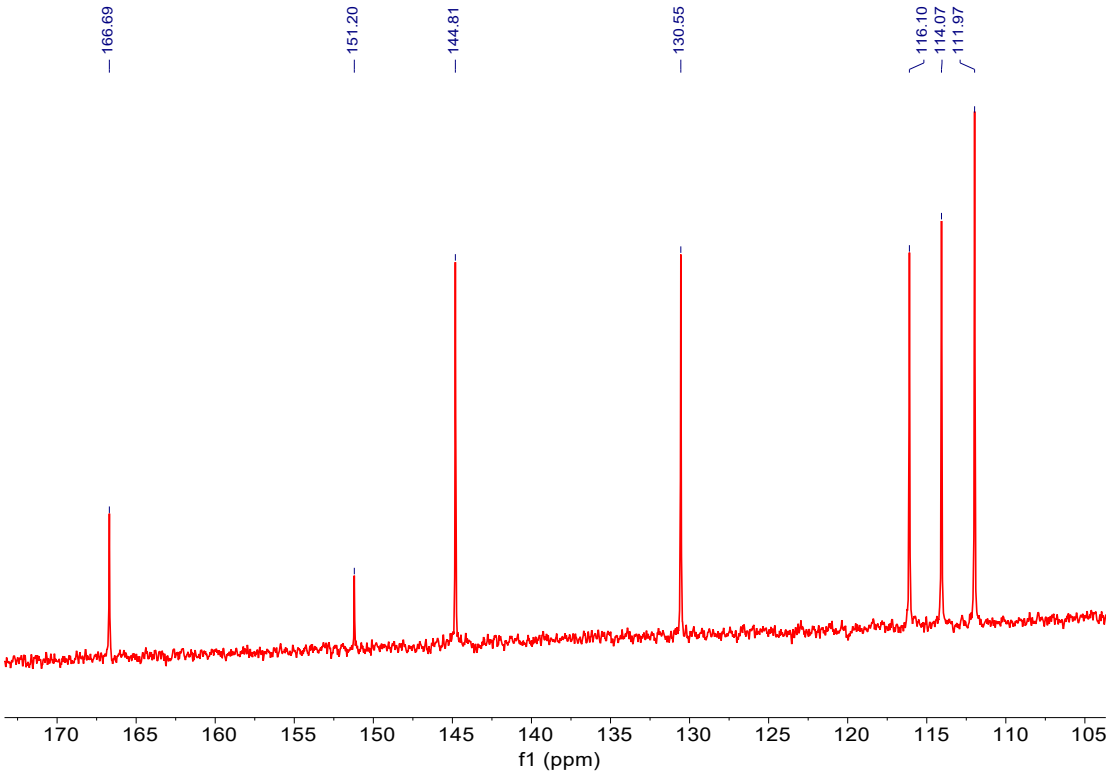

Figure S3. ^{13}C NMR of furylacrylic acid (100 MHz, $CDCl_3$)

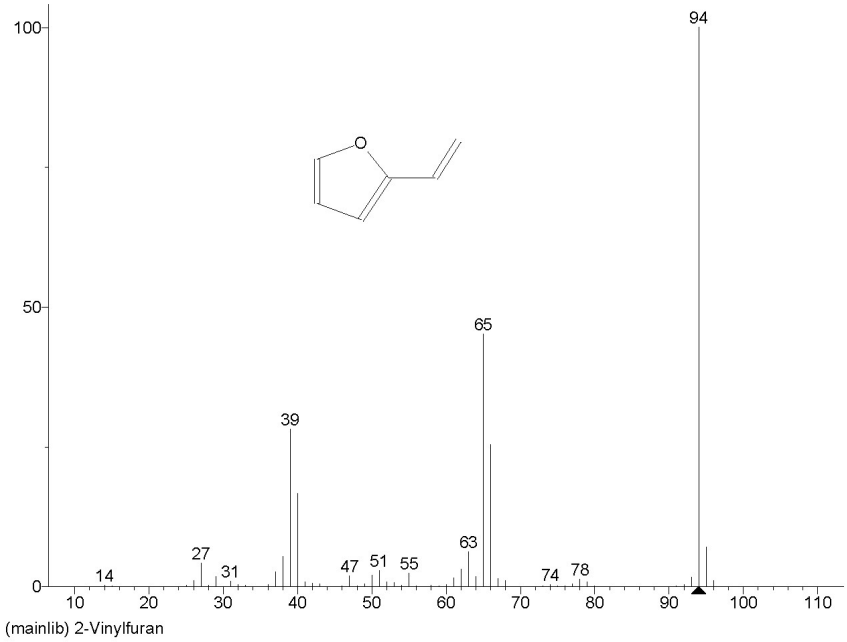

Figure S4. Mass spectrum fragmentation pattern of 2-vinylfuran

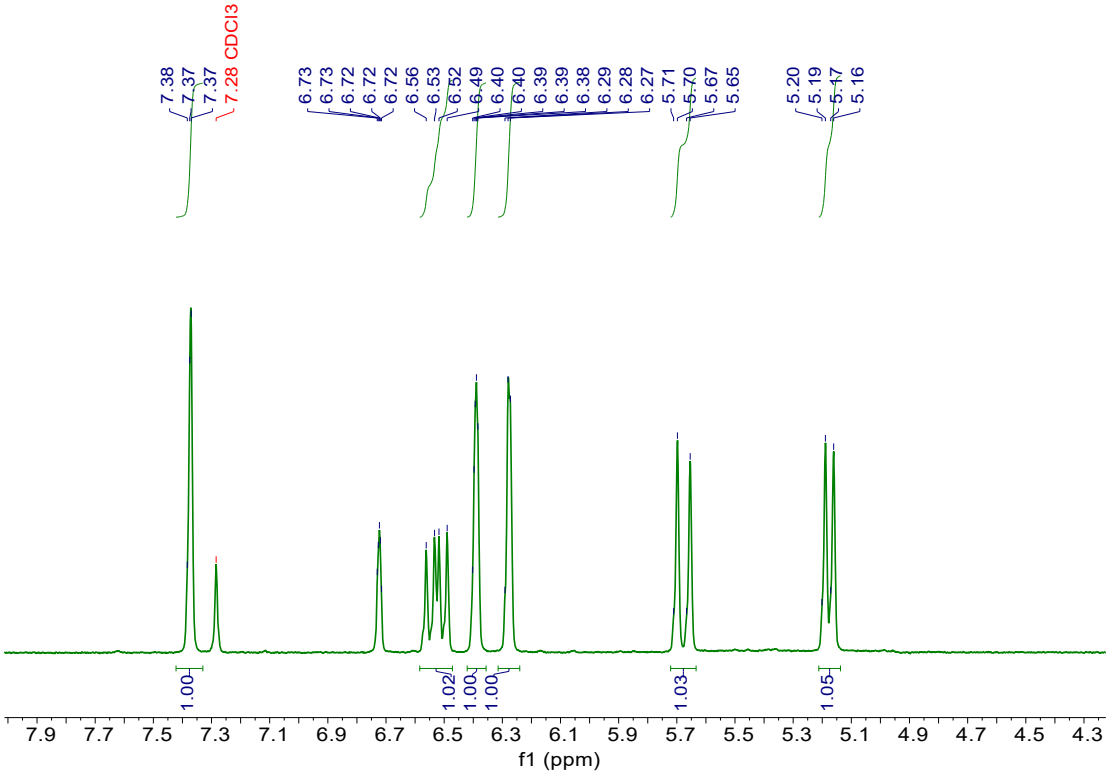

Figure S5. ^{1}H NMR of 2-vinylfuran (400 MHz, $CDCl_3$)

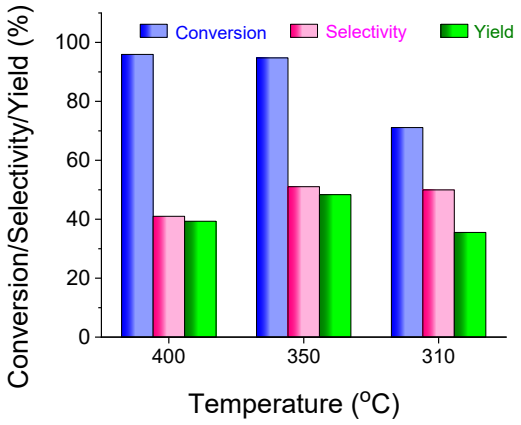

Figure S6. Catalytic results versus reaction temperature over Na/SiO_2

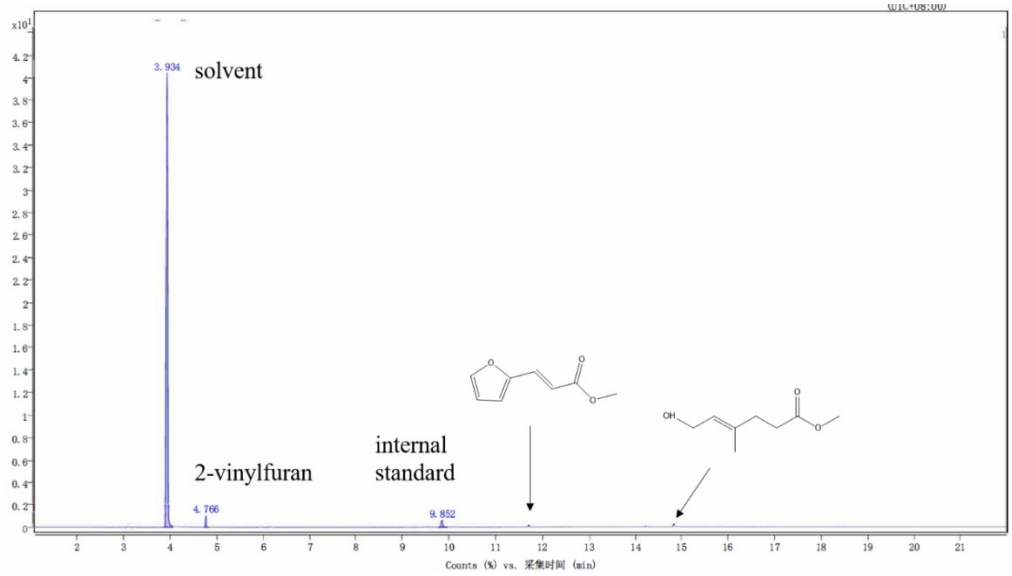

Figure S7. Outlet products of furylacrylic acid decarboxylation. (Others, unkown compounds)

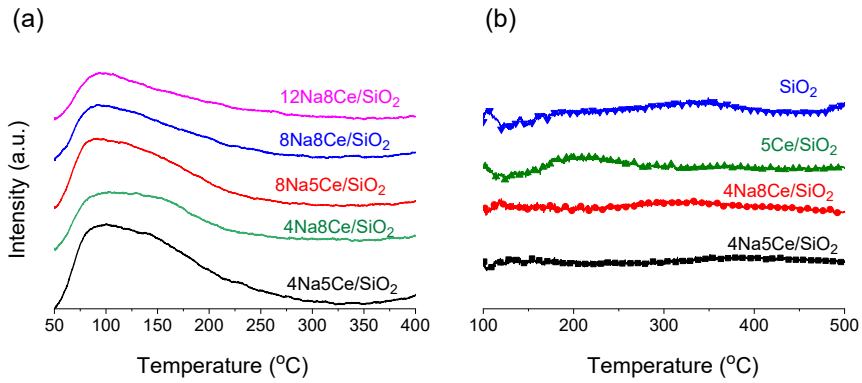

Figure S8. (a) CO_2-TPD and (b) NH_3-TPD profiles. The results suggested that these catalysts had many basic sites and trace acidic sites, indicating that the basic sites may correspond to the active sites.

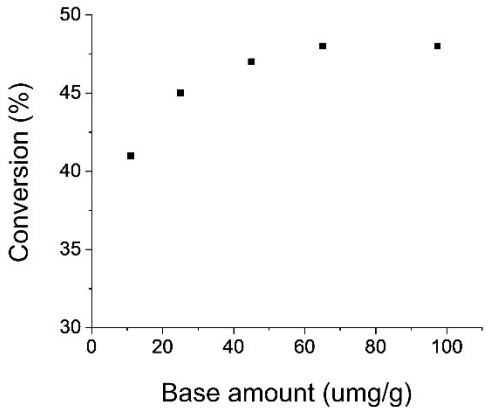

Figure S9. Correlation between base amount and conversion

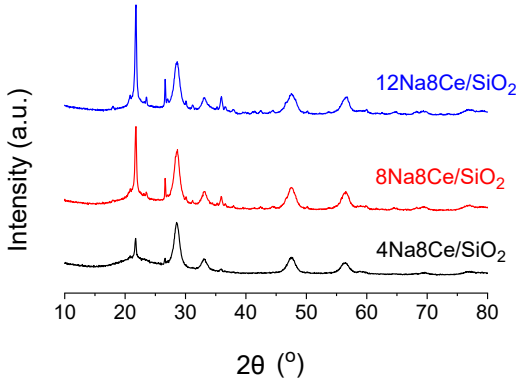

Figure S10. XRD pattern of the catalysts.

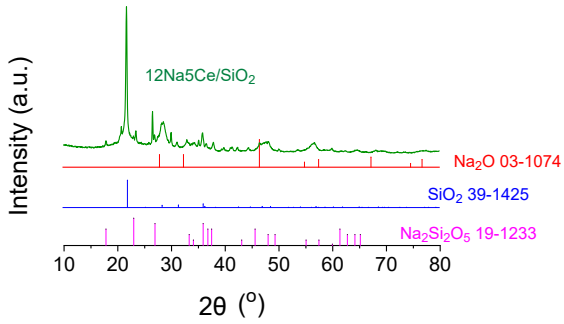

Figure S11. XRD pattern of 12Na5Ce/SiO_2 and the standard PDF cards of Na_2O (JCPDS PDF#03-1074), SiO_2 (JCPDS PDF#39-1425), and $Na_2Si_2O_5$ (JCPDS PDF#19-1233).

Table S1 Textural properties of the catalysts

Sample	BET			ICP		
	Surface area (m^2/g)	Pore size (nm)	Pore volume (cc g^{-1})	Na wt%	Ce wt%	Na/Ce (atom ratio)
4Na5Ce/SiO_2	85.24	18.73	0.49	4.2	4.3	5.94
8Na5Ce/SiO_2	22.62	22.68	0.15	7.7	4.3	10.90
12Na5Ce/SiO_2	15.75	22.69	0.10	12.0	4.7	16.99
4Na8Ce/SiO_2	81.11	15.12	0.45	4.3	8.4	6.09
8Na8Ce/SiO_2	20.93	22.63	0.14	7.8	8.1	11.04

$12Na8Ce/SiO_2$	11.27	3.41	0.05	10.7	8.0	15.15
$5Ce/SiO_2$	298.49	8.38	0.99	-	4.4	-
$8Ce/SiO_2$	324.49	8.38	0.10	-	8.5	-

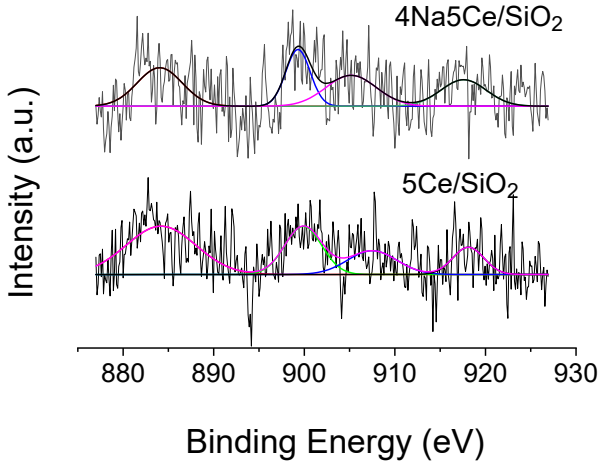

Figure S12. XPS of Ce 3d of $5Ce/SiO_2$ and $4Na5Ce/SiO_2$.

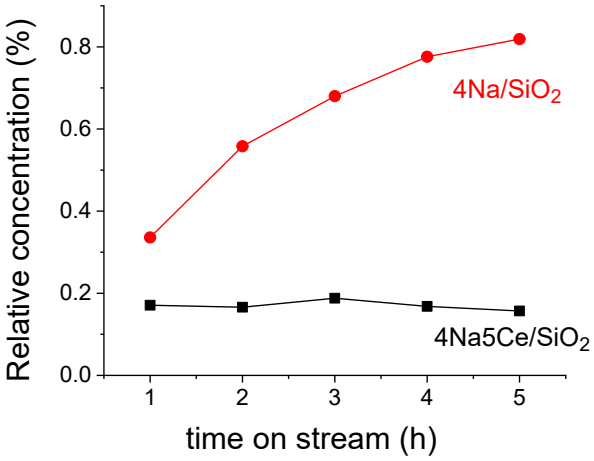

Figure S13. Byproducts formation versus time on stream over $4Na/SiO_2$ and $4Na5Ce/SiO_2$.

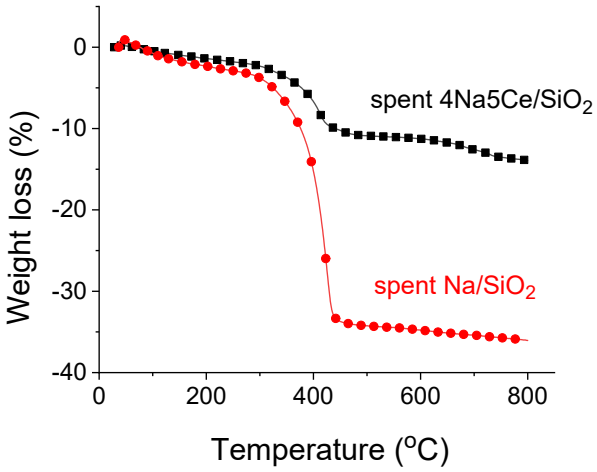

Figure S14. TGA curves of spent 4Na5Ce/SiO_2 and spent Na/SiO_2.

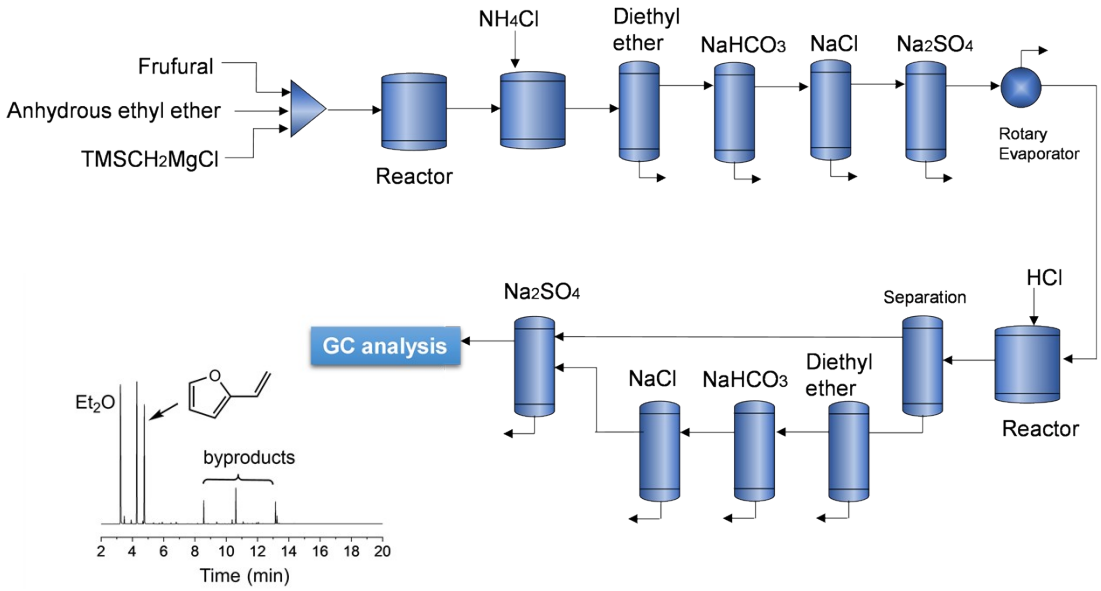

Figure S15. Process flow diagram for 2-vinylfuran production by using route 1 (reported approach), and GC analysis of the obtained products.

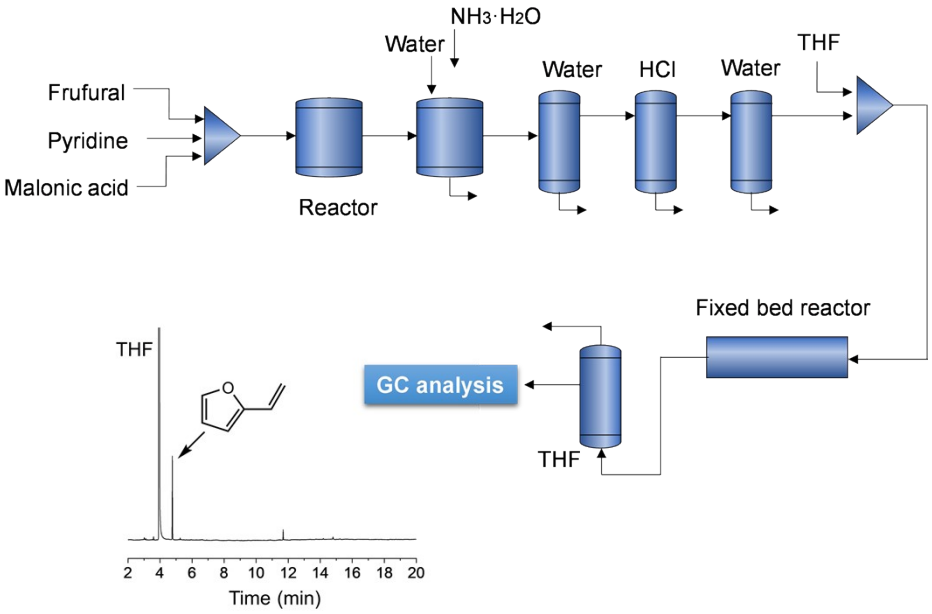

Figure S16. Process flow diagram for 2-vinylfuran production by using route 2 (our approach), and GC analysis of the obtained products.

Table S2. Process flow diagram for 2-vinylfuran production by using route 1 (reported approach)

Unit	Reagent	Consumption	Reagent cost (¥)	Temperature (°C)	Time (h)
1	Furfural	5ml	3.75	0	5
	Dried Et_2O	60ml	25.92	RT	14
	$TMSCH_2MgCl$	50ml	67	RT	
2	Saturated NH_4Cl	40ml	0.2	0	0.4
3	Et_2O	50ml×2	30	RT	0.8
	Separation			RT	
4	Saturated $NaHCO_3$	30ml×2	0.3	RT	0.4
5	Brine	30ml×2	0.3	RT	
6	Na_2SO_4	3g	0.1	RT	0.1
7	Removal solvent			30	0.5
8	Et_2O	20ml	6	RT	
	HCl	2g	0.1	RT	10

9	Separation				
10	Extraction (Et_2O)	20ml×2	12	RT	0.5
11	Saturated $NaHCO_3$	20ml	0.1	RT	
12	Brine	20ml	0.1	RT	0.3
	Separation				
13	Na_2SO_4	3g	0.1	RT	0.2

Yield 69%; Energy cost 7.5 ¥; others 2 ¥.

Table S3 Process flow diagram for 2-vinylfuran production by using route 2 (our approach)

Unit	Reagent	Consumption	Temperature (°C)	Reagent cost (¥)	Time (h)
1	Furfural	5ml	100	3.75	2.5
	Malonic acid	6.26ml		1.56	
	Pyridine	2.9ml		0.3	
2	DI water	6ml	RT		0.8
	Ammonia	25ml		0.35	
3	Water	2.4ml	RT		2
4	HCl	10g	RT	0.5	
5	Separation				
	Furylacrylic acid	yield 95%			
6	THF	120ml		7.2	
7	Fixed reactor		350		19
	Catalyst	1.6g		0.25	5
8	THF	20ml×12		15	

Yield 89%; Energy cost 39 ¥; others 10 ¥.

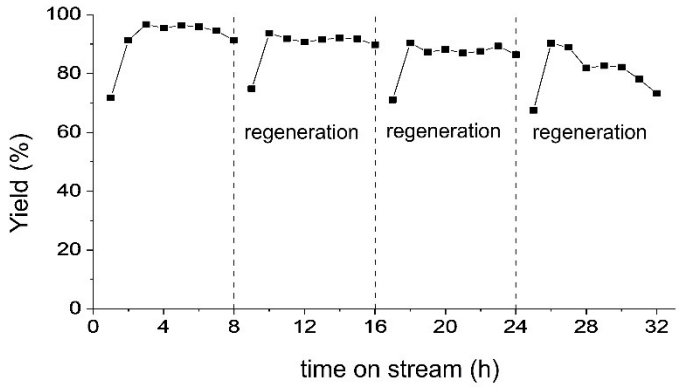

Figure S17 Catalytic results versus time on stream over 4Na5Ce/SiO_2. The catalyst regeneration was conducted out in fixed bed reactor under an air flow of 90 ml/min at 550 ℃ for 4h.

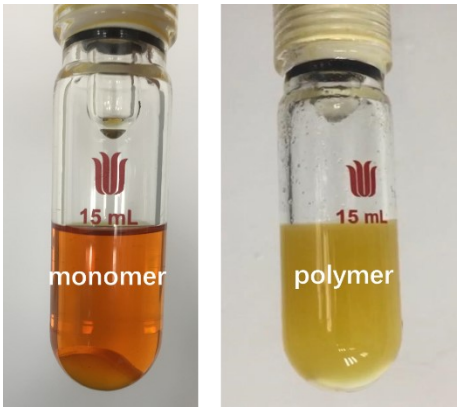

Figure S18. Photograph of reaction system: before (left) and (right) after polymerization

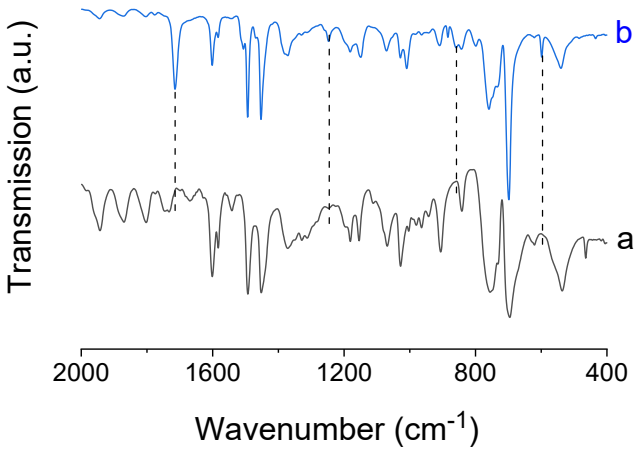

Figure S19. IR of polystyrene (a) and (b) 2-vinylfuran based polymer

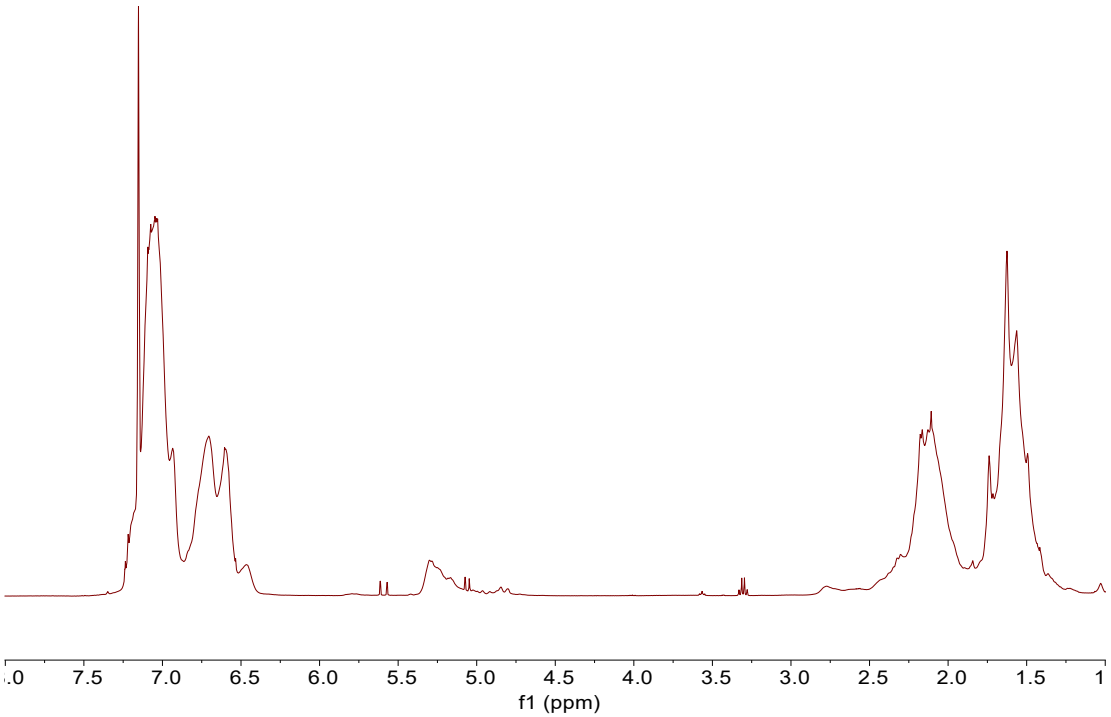

Figure S20. ^{1}H NMR of polystyrene (400MHz, $CDCl_3$)

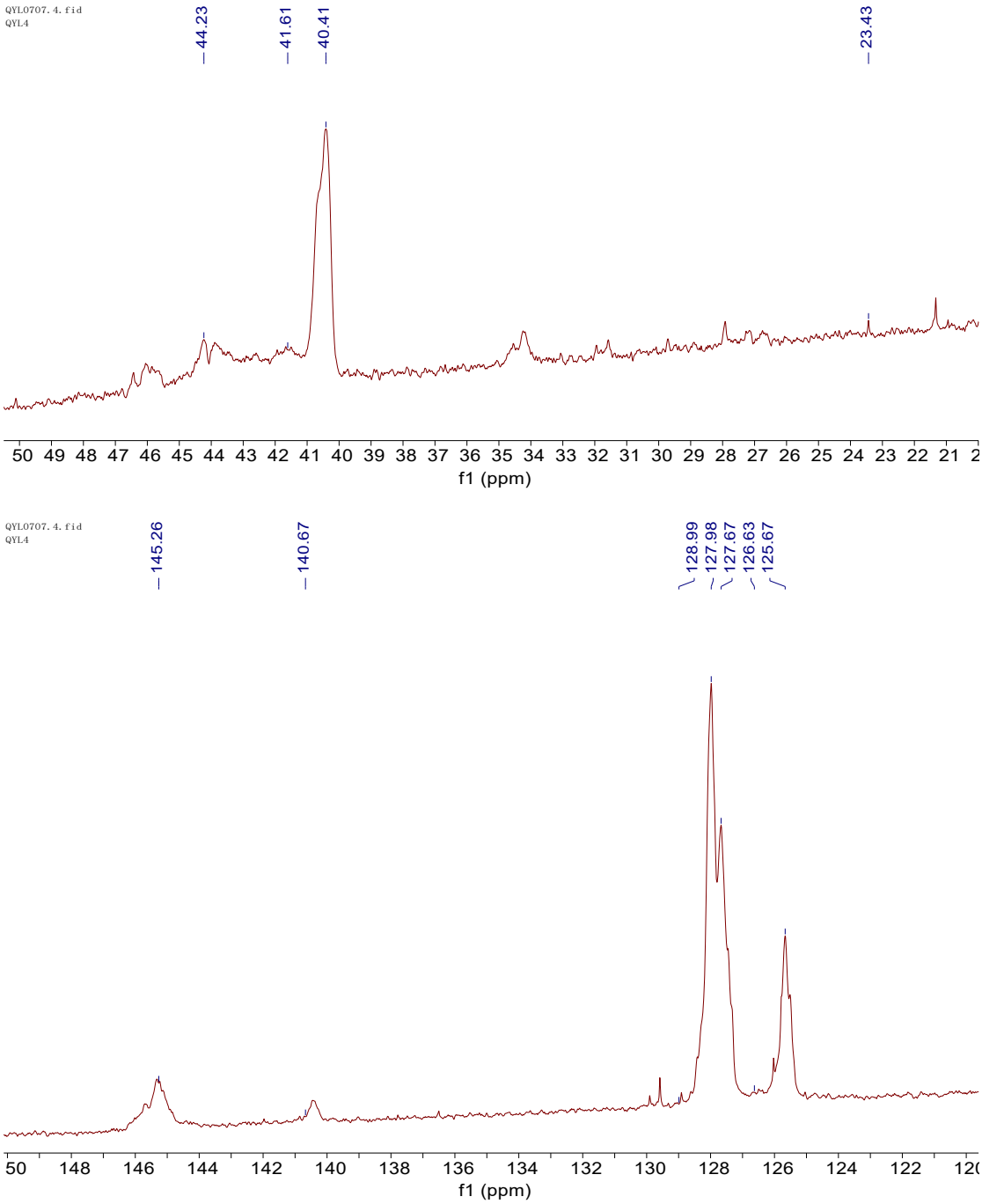

Figure S21. ^{13}C NMR of polystyrene (100MHz, $CDCl_3$)

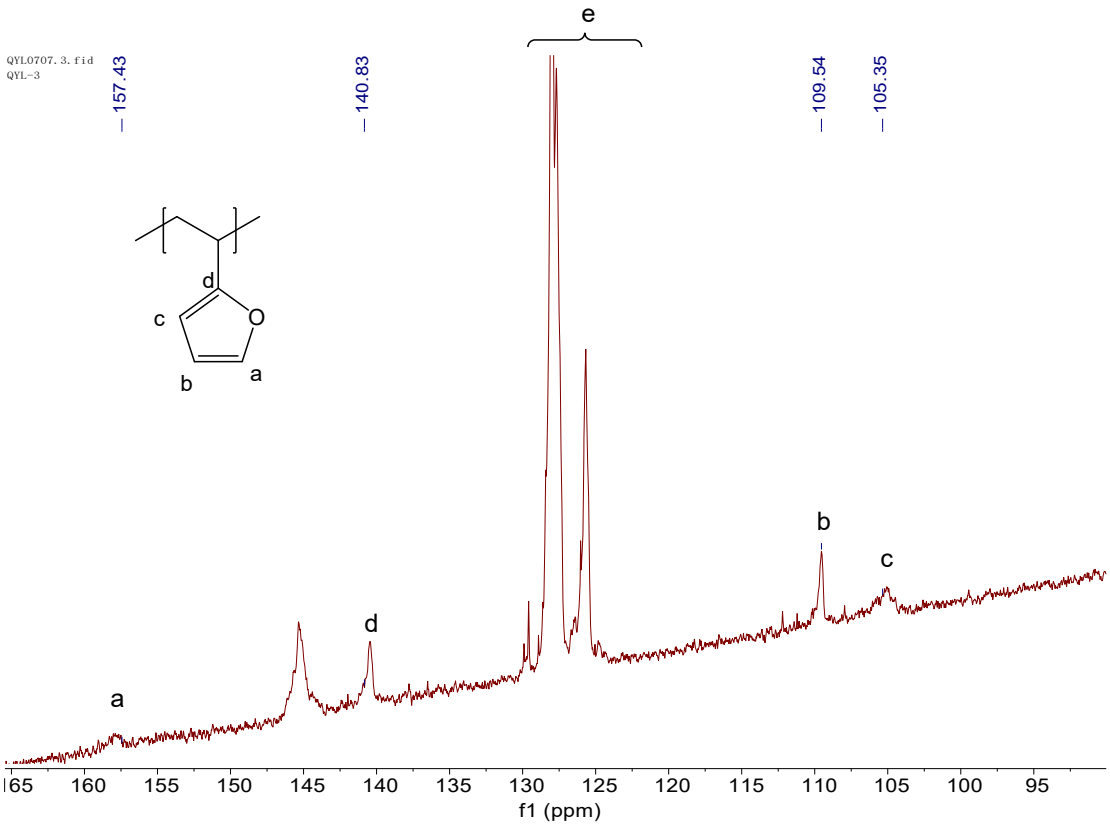

Figure S22. ^{13}C NMR of 2-vinylfuran based polymer (100MHz, $CDCl_3$). The peaks (e) at 125~130 ppm were associated with polystyrene.[3, 4]

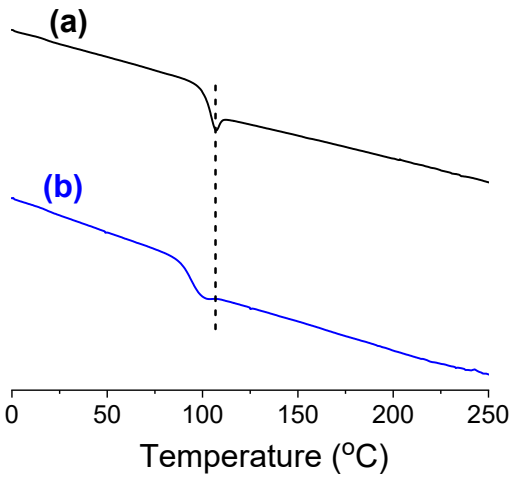

Figure S23. DSC: (a) polystyrene, (b) 2-vinylfuran based polymer

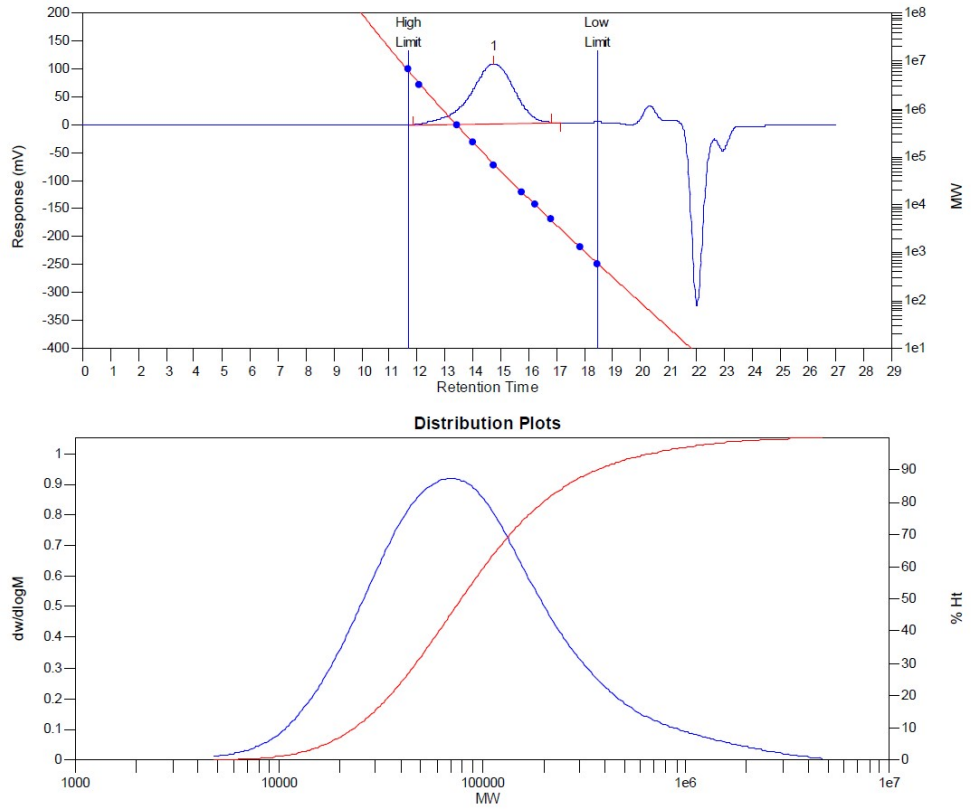

Figure S24. GPC of polystyrene. Mn=50378, DPI=3.30

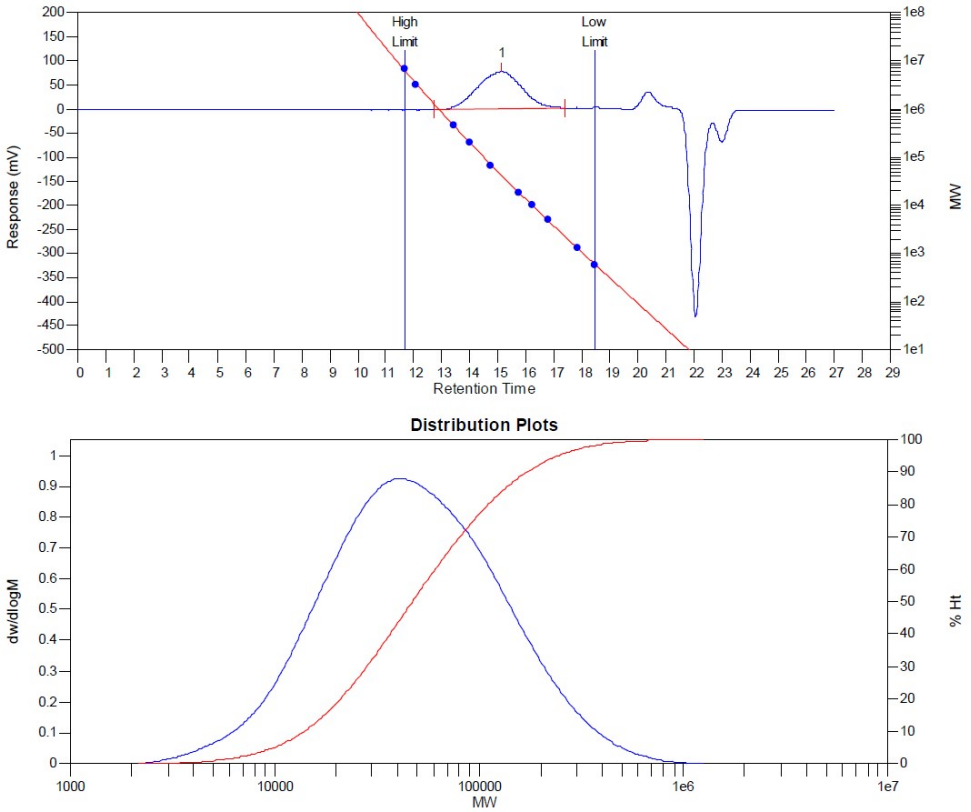

Figure S25. GPC of 2-vinylfuran based polymer. Mn=29336, DPI=2.50

References

[1] O. Kikhtyanin, L. Čapek, L. Smoláková, Z. Tišler, D. Kadlec, M. Lhotka, P. Diblíková, D. Kubička, Influence of Mg–Al Mixed Oxide Compositions on Their Properties and Performance in Aldol Condensation, Ind. Eng. Chem. Res., 56 (2017), pp. 13411-13422. https://doi.org/10.1021/acs.iecr.7b03367

[2] O.V. Larina, P.I. Kyriienko, N.D. Shcherban, P.S. Yaremov, D.Y. Balakin, I. Khalakhan, K. Veltruská, S.O. Soloviev, S.M. Orlyk, Carbon-Supported Mg–Al Oxide Hybrid Catalysts for Aqueous Ethanol Conversion into 1-Butanol in a Flow Reactor, Ind. Eng. Chem. Res., 60 (2021), pp. 11964-11976. https://doi.org/10.1021/acs.iecr.1c02153

[3] S. Long, F. Lin, C. Yao, D. Cui, Highly cis-1,4 Selective Living Polymerization of Unmasked Polar 2-(2-Methylidenebut-3-enyl)Furan and Diels–Alder Addition, Macromol. Rapid Commun., 38 (2017), pp. 1700227. https://doi.org/10.1002/marc.201700227

[4] F. Lin, Z. Liu, M. Wang, B. Liu, S. Li, D. Cui, Chain Transfer to Toluene in Styrene Coordination Polymerization, Angew. Chem. Int. Ed., 59 (2020), pp. 4324-4328. https://doi.org/10.1002/anie.201914603